The optical companion to the binary millisecond pulsar J1824-2452H in the globular cluster M28[1]

C. Pallanca[2], E. Dalessandro[2], F.R. Ferraro[2], B. Lanzoni[2], R.T. Rood[3], A. Possenti[4], N. D'Amico[4,5], P.C. Freire[6], I. Stairs[7], S.M. Ransom[8], S. Bégin[7,9],

[2] *Dipartimento di Astronomia, Università degli Studi di Bologna, via Ranzani 1, I–40127 Bologna, Italy*

[3] *Astronomy Department, University of Virginia, P.O. Box 3818, Charlottesville, VA 22903-0818, USA*

[4] *INAF-Osservatorio Astronomico di Cagliari, località Poggio dei Pini, strada 54, I-09012 Capoterra, Italy*

[5] *Dipartimento di Fisica, Università di Cagliari, Cittadella Universitaria, I-09042 Monserrato, Italy*

[6] *Max-Planck-Institut für Radioastronomie, Auf dem Hügel 69, D-53121 Bonn, Germany*

[7] *Department of Physics and Astronomy, University of British Columbia, 6224 Agricultural Road, Vancouver, BC, V6T 1Z1, Canada*

[8] *National Radio Astronomy Observatory, Charlottesville, VA 22903, USA*

[9] *Département de physique, de génie physique et d'optique, Université Laval, Québec, QC, G1K 7P4, Canada*

8 October, 2010

ABSTRACT

We report on the optical identification of the companion star to the eclipsing millisecond pulsar PSR J1824-2452H in the galactic globular cluster M28 (NGC 6626). This star is at only $0.2''$ from the nominal position of the pulsar and it shows optical variability (~ 0.25 mag) that nicely correlates with the pulsar orbital period. It is located on the blue side of the cluster main sequence, ~ 1.5 mag fainter than the turn-off point. The observed light curve shows two distinct and asymmetric minima, suggesting that the companion star is suffering tidal distortion from the pulsar. This discovery increases the number of non-degenerate MSP companions optically identified so far in globular clusters (4 out of 7), suggesting that these systems could be a common outcome of the pulsar recycling process, at least in dense environments where they can be originated by exchange interactions.

Subject headings: Binaries: close – globular clusters: individual (M28) – pulsars: individual (PSR J1824−2452H) – stars: evolution – stars: neutron

1. INTRODUCTION

The ultra-dense cores of globular clusters (GCs) are very efficient "furnaces" for generating exotic objects, such as low-mass X-ray binaries, cataclysmic variables, millisecond pulsars (MSPs), and blue stragglers (e.g., Bailyn 1995; Verbunt et al. 1997; Ferraro et al. 2001a). Most of these objects are thought to be the result of the evolution of various kinds of binary systems originated and/or hardened by stellar interactions (e.g., Clark 1975; Hills & Day 1976; Bailyn 1992; Ferraro et al. 1995). The nature and even the existence of binary by-products are strongly related to the cluster core dynamics (e.g. Heggie 1975, Ivanova et al. 2008). Hence they may be very useful diagnostics of the dynamical evolution of GCs (e.g., Goodman & Hut 1989; Hut et al. 1992; Meylan & Heggie 1997; Pooley et al. 2003; Fregeau 2008; Ferraro et al. 2009a).

In particular, MSPs are formed in binary systems containing a slowly rotating neutron star (NS) that is eventually spun up to millisecond periods by heavy mass accretion from an evolving companion, that, in turn, is expected to become a white dwarf (WD; e.g. Lyne et al. 1987; Alpar et al. 1982; Bhattacharya & van den Heuvel 1991). More than 50% of known MSPs are found in GCs, although the Galaxy mass is 100 times larger than that of the whole GC system. While this is partially due to the deeper investigations performed in GCs with respect to the field, it very likely indicates that dynamics plays a significant role in the formation of these objects. In fact, in the ultra-dense GC cores, dynamical interactions can promote the formation of binaries suitable for recycling NSs into MSPs (e.g., Davies & Hansen 1998), while in the Galactic field the only viable formation channel for MSPs is the evolution of primordial binaries. The optical identification of the companion stars to binary MSPs is a fundamental step for characterizing these systems and for clarifying the possible recycling mechanisms. In the case of GCs, it also represents a crucial tool for quantifying the occurrence of dynamical interactions, understanding the effects of crowded stellar environments on the evolution of binaries, determining the shape of the GC potential well, and estimating the mass-to-light ratio in the GC cores (e.g., Phinney 1992; Possenti et

[1]Based on observations with the NASA/ESA HST, obtained at the Space Telescope Science Institute, which is operated by AURA, Inc., under NASA contract NAS5-26555. Also based on observations collected at the European Southern Observatory at La Silla (Chile) with the MPI Telescope under program 164.O-0561(F)

al. 2003; Ferraro et al. 2003a).

Despite their importance, up to now only six optical counterparts to MSP companions have been identified in five GCs. In the colour-magnitude diagram (CMD) three of them have positions consistent with the cooling sequences of helium WDs, in agreement with the expectations of the MSP recycling scenario. These are the companions to MSP-U in 47 Tucanae (Edmonds et al. 2001); MSP-A in NGC 6752 (Ferraro et al. 2003b), and PSR B1620-26 in M4 (Sigurdsson et al. 2003). The other identified companions show, instead, quite peculiar properties. The luminosity and colours of the optical companion to MSP-A in NGC 6397 are totally incompatible with those of a WD. This is a relatively bright, tidally deformed star, suggesting that the system either harbours a newly born MSP, or is the result of an exchange interaction (Ferraro et al. 2001b). The companion star to MSP-B in NGC 6266 is a similarly bright object, with luminosity comparable to the cluster main sequence (MS) turn-off, an anomalous red colour and optical variability suggestive of a tidally deformed star which filled its Roche Lobe (Cocozza et al. 2008). This object is also a Chandra X-ray source, thus supporting the hypothesis that some interaction is occurring between the pulsar wind and the gas streaming off the companion. Finally the companion to MSP-W in 47 Tuc has been identified to be a faint MS star, showing large-amplitude, sinusoidal luminosity variations probably due to the heating effect of the pulsar (Edmonds et al. 2002).

As a part of a project aimed to perform a systematic search for optical companions to binary MSPs in GCs (see Ferraro et al. 2001b, Ferraro et al. 2003b, Cocozza et al. 2008), here we focus our attention on M28 (NGC 6626). M28 is a Galactic GC with intermediate central density ($\log \rho_0 = 4.9$ in units of $M_\odot/\mathrm{pc}^3$; Pryor & Meylan 1993). It is the first GC where a MSP was discovered (Lyne et al. 1987) and to date it is known to harbour a total of twelve pulsars (Bégin 2006). This is the third largest population of known pulsars in GCs, after that of Terzan 5 (with 33 objects; Ransom et al. 2005, but see the recent results by Ferraro et al. 2009b and Lanzoni et al. 2010, suggesting that Terzan 5 is not a genuine GC) and that of 47 Tuc (with 23 MSPs; Camilo et al. 2000; Freire et al. 2003).[2]

Among the binary MSPs harboured in M28, J1824-2452H (hereafter M28H) deserves special attention since it is an eclipsing system showing a number of timing irregularities, possibly due to the tidal effect on the companion star (Bégin 2006; Stairs et al. 2006). It is located at $\alpha_{2000} = 18^{\mathrm{h}}24^{\mathrm{m}}31.61^{\mathrm{s}}$ and $\delta_{2000} = -24^\circ 52' 17.2''$, it has an orbital period $P = 0.43502743$ days and shows eclipses for $\sim 20\%$ of it (S. Bégin et al. 2010, in preparation). There is also an associated X-ray source, possibly variable at the binary period and with

[2]See the complete list of pulsars in GCs at http://www.naic.edu/∼pfreire/GCpsr.html

a hard spectrum (Bogdanov et al. 2010). Such X-ray emission is likely due to the shock between the MSP magnetospheric radiation and the matter released by the companion, like that detected in the case of MSP-W in 47 Tuc (Bogdanov et al. 2005). This further suggests that the companion star to M28H is a non-degenerate star. In this letter we present its optical identification, based on high-quality, phase-resolved photometry obtained with the new Wide Field Camera 3 (WFC3) on board the Hubble Space Telescope (HST).

2. OBSERVATIONS AND DATA ANALYSIS

The photometric data-set used for this work consists of HST high-resolution images obtained with the ultraviolet-visible (UVIS) channel of the WFC3. A set of supplementary HST Wide Field Planetary Camera 2 (WFPC2) images, and ground-based wide-field images obtained at the European Southern Observatory (ESO) have been retrieved from the Science Archive and used for variability and astrometric purposes.

The WFC3 UVIS CCD consists of two twin detectors with a pixel-scale of $\sim 0.04''$/pixel and a global field of view (FOV) of $\sim 162'' \times 162''$. The WFC3 images have been obtained on 2009 August 8 (Prop. 11615, P.I. Ferraro) in four different bands. The data-set consists of: 6 images obtained through the F390W filter ($\sim U$) with an exposure time of $t_{\rm exp} = 800 - 850$ sec each; 7 images in F606W ($\sim V$) with $t_{\rm exp} = 200$ sec; 7 images in F814W ($\sim I$) with $t_{\rm exp} = 200$ sec; and 7 images in F656N (a narrow filter corresponding to Hα) with exposure time ranging from $t_{\rm exp} = 935$ sec, up to $t_{\rm exp} = 1100$ sec. All the images are aligned and the cluster is almost centered in CHIP1.

Additional public WFPC2 images have been retrieved from the archive. The first data-set (hereafter WFPC2-A) was obtained in 1997 (Prop. 6625) and consists of 8 images in F555W ($\sim V$) with $t_{\rm exp} = 140$ sec and 9 images in F814W ($6 \times t_{\rm exp} = 160$ sec and $3 \times t_{\rm exp} = 180$ sec). The second sample (hereafter WFPC2-B) consists of 13 images in F675W ($\sim R$), with $t_{\rm exp} = 100$ sec each, secured in 2008 (Prop. 11340).

Finally, the wide-field data-set consists of 6 images in the V and I filters, obtained in August 2000 with the Wide Field Imager (WFI) at the ESO-MPI 2.2 m telescope (La Silla, Chile). The WFI consists of a mosaic of eight chips, for a global FOV of $34' \times 34'$.

The data reduction procedure (all the details will be discussed in a forthcoming paper; E. Dalessandro et al. 2010, in preparation) has been performed on the WFC3 "flat fielded" (flt) images, once corrected for "Pixel-Area-Map" (PAM) by using standard IRAF procedures. The photometric analysis has been carried out by using the DAOPHOT package (Stetson 1987). For each image we modeled the point spread function (PSF) by using a large number

(~ 200) of bright and nearly isolated stars. Then we performed the PSF fitting by using the DAOPHOT packages ALLSTAR and ALLFRAME (Stetson 1987, 1994). The final star list consists of all the sources detected in at least 14 frames on a total number of 27. A similar procedure has been adopted to reduce the WFPC2 images. For the WFPC2-A data-set we demanded that sources were in at least 9 frames out of 17, whereas for the WFPC2-B data-set in at least 7 frames out of 13. Since the WFC3 images heavily suffer from geometric distortions within the FOV, we corrected the instrumental positions of stars by applying the equations reported by Bellini & Bedin (2009) for the filter F336W, neglecting any possible dependence on the wavelengths. Standard procedure (see e.g., Lanzoni et al. 2007) has been adopted to analyze the WFI data. Here we use this data-set only for astrometric purposes. In fact, very accurate astrometry is the most critical task in searching for the optical counterparts to MSPs, especially in crowded fields such as the central regions of GCs, where primary astrometric standards are lacking (e.g., Ferraro et al. 2001a, 2003b). For this reason we first placed the wide-field catalog obtained from the WFI images on the absolute astrometric system, and we then used the stars in common with the high resolution data-sets as secondary standards. In particular, the WFI catalogue has been reported onto the coordinate system defined by the Guide Star Catalogue II (GSCII) through cross-correlation. Then, we placed the WFC3 and the WFPC2 catalogues on the same system through cross-correlation with the WFI data-set. Each transformation has been performed by using several thousand stars in common, and at the end of the procedure the typical accuracy of the astrometric solution was $\sim 0.2''$ in both right ascension (α) and declination (δ).

Finally, the WFC3 instrumental magnitudes have been calibrated to the VEGAMAG system by using the photometric zero-points and the procedures reported on the WFC3 web page.[3] The WFPC2 magnitudes have been reported to the same photometric system by using the procedure described in Holtzman et al. (1995), with the gain settings and zero-points listed in Tab. 28.1 of the HST data handbook.

3. THE OPTICAL COMPANION TO M28H

In order to search for the optical counterpart to the M28H companion, we carefully re-analyzed a set of $4'' \times 4''$ WFC3 sub-images centered on the nominal radio position of the MSP. For these sub-images the photometric reduction has been re-performed by using both DAOPHOT (Stetson 1987) and ROMAFOT (Buonanno et al. 1983). In both cases, in order to optimize the identification of faint objects, we performed the source detection on the

[3]http://www.stsci.edu/hst/wfc3/phot_zp_lbn

median image in the U band, thus obtaining a master-list. The master-list was then applied to all the single images in each band and we performed the PSF-fitting by using appropriate PSF models obtained in each image. The resulting instrumental magnitudes were reported to those of a reference image in each filter, and from the frame-to-frame scatter, a mean magnitude and a standard deviation have been obtained for all the objects.

We then selected the stars that showed significant variations in the U band, looking for those that have a periodic variability compatible with the orbital period of M28H. Only one object has been found to match such requirements. This star is located at $\alpha_{2000} = 18^{\rm h}24^{\rm m}31.60^{\rm s}$ and $\delta_{2000} = -24°52'17.2''$, just $0.17''$ from the radio position of M28H, and $\sim 0.4''$ from the X-ray source (Figure 1).

In order to carefully investigate the optical modulation of this star, we first folded all the measured datapoints obtained in each filter by using the orbital period P and the reference epoch ($T_0 = 53755.226397291$ MJD; Bégin et al. 2010) of the M28H radio ephemeris. Since the few measured datapoints in the single bands are not sufficient to properly cover the entire period (see dots in Fig. 2), we computed the average magnitude in each filter and the shift needed to make it match the mean U-band magnitude, which we adopted as a reference. We thus obtained the combined light curve shown in Figure 3, which well samples the entire period of variation. Indeed, the optical modulation of the identified star nicely agrees with the orbital period of the MSP, thus fully confirming that the variability is associated with the pulsar binary motion. Hence we conclude that the identified star (hereafter COM-M28H) is the optical companion to M28H.

This object (with $U = 21.99$, $V = 20.58$, $I = 19.49$) is ~ 1.5 mag fainter than the cluster turn-off and slightly bluer than the MS (Figure 4). Clearly, it is far too red and bright to be compatible with a WD (the recycling by-product expected from the standard scenario). Instead, its position in the CMD is marginally consistent with a MS star. In particular, the cluster MS is well reproduced by a $t = 13$ Gyr isochrone (from Marigo et al. 2008), with metallicity [Fe/H]$= -1.27$ (from Zinn 1980, after calibration to the scale of Carretta & Gratton 1997, following Ferraro et al. 1999) and assuming a color excess $E(B-V) = 0.4$ and a distance modulus $(\text{m-M})_V = 14.97$ (Harris 1996). By projecting the observed magnitudes and colours of COM-M28H onto this isochrone, the resulting mass, temperature and radius would be $M_{\rm COM} \sim 0.68 M_\odot$, $T \sim 6000$ K, $R \sim 0.64 R_\odot$, respectively. However these quantities should be considered as just an indication, since the observational properties of this object (see below) strongly suggest that it is a highly perturbed star.

Since the two WFPC2 data-sets have been obtained in two different epochs with a time baseline of more than 10 years, and given the relative small distance of M28 (d=5.6 Kpc; Harris 1996), we have been able to perform a proper-motion analysis. As shown in

Figure 5, the bulk of stars lie around the position ($\mu_\alpha cos(\delta) = 0$, $\mu_\delta = 0$) [mas/yr], within a radius $\sigma_\mu \sim 1$. These most likely are members of the cluster, while field stars are clearly separated (the position in the CMD of these two classes of stars further confirms such a conclusion; Dalessandro et al. 2010). Since no extra-galactic source can be identified in the FOV adopted for this analysis, no absolute proper motion determination can be obtained. However a rough estimate can be derived by averaging the positions of field stars: we obtain $\mu_\alpha cos(\delta) = -1.40$ and $\mu_\delta = 3.50$) [mas/yr], in agreement with previous results (Cudworth & Hanson 1993). COM-M28H lies at ($\mu_\alpha cos(\delta) = -0.09 \pm 0.15$, $\mu_\delta = 0.09 \pm 0.15$) [mas/yr], thus fully behaving as a member of the cluster.

4. DISCUSSION

The observed light curve of COM-M28H (Fig. 3) clearly shows two distinct and asymmetric minima, at phases $\phi \sim 0.25$ and $\phi \sim 0.75$, quite similar to what is observed for two other MSP companions (Ferraro et al. 2001b; Cocozza et al. 2008). Such a shape is a clear signature of ellipsoidal variations induced by the NS tidal field on a highly perturbed, bloated star. Moreover, the relative deepness of the two minima (consistent with a light curve purely due to ellipsoidal variations) suggests that only a marginal (if any) over-heating is affecting the side of the companion facing the pulsar. This is also supported by the non-detection of H_α emission from the system (see the right panel of Fig. 4).

Given the mass function derived from the radio observations ($f_1 = 0.00211277 M_\odot$; Bégin 2006), and assuming $1.4 M_\odot$ for the MSP mass and $0.68 M_\odot$ for the mass of COM-M28H (as derived from the cluster best-fit isochrone), the resulting orbital inclination of the system would be $i \sim 18°$. Such a low value for the inclination angle would not produce any optical modulation. Indeed both the light curve shape and the occurrence of eclipses in the radio signal point toward a significantly higher value of the orbital inclination (which corresponds to a lower companion mass for a given mass function). By assuming $i = 60°$ (the median of all possible inclination angles) a companion mass of $\sim 0.2 M_\odot$ is obtained. In this configuration the corresponding total mass of the system would be $M_{\rm T} = 1.6 M_\odot$ and the physical orbital separation of the system is $a \sim 2.8 R_\odot$. In order to check whether such a configuration reproduces the observed light curve, we employed the publicly available software NIGHTFALL.[4]. We fixed the orbital period of the pulsar to the radio value and the surface temperature of COM-M28H to $T = 6000$ K (as inferred from the position in the CMD). We then used an iterative procedure letting the orbital inclination, the mass ratio

[4]Available at http://www.hs.uni-hamburg.de/DE/Ins/Per/Wichmann/Nightfall.html.

($M_{\rm NS}/M_{\rm COM}$) and the Roche Lobe filling factor vary respectively in the ranges $0^\circ - 90^\circ$, $1 - 20$, and $0.1 - 1$. By using as selection criterion a χ^2 test, the best-fit model (Figs. 2 and 3) was obtained for an inclination $i \simeq 65^\circ$, a mass ratio $M_{\rm NS}/M_{\rm COM} \simeq 7$ and a Roche Lobe filling factor equal to 1. These results confirm that a configuration with a highly distorted companion of about $0.2M_\odot$, orbiting a $1.4M_\odot$ MSP, in a plane with an orbital inclination of $\sim 60 - 70^\circ$ well reproduces both the mass function of the system derived from the radio observations, and the optical light curve of COM-M28H. It is worth noticing that a good fit can be obtained only if COM-M28H completely filled its Roche Lobe, which, following Paczynski (1971), we estimate to be $\sim 0.65R_\odot$. While such a large value of the stellar radius allows to account for the observed luminosity of COM-28H,[5] it is far too small to cause the observed radio eclipse. In fact an eclipse lasting for $\sim 20\%$ of the orbital period corresponds to an eclipsing region of $\sim 3.3R_\odot$ size. This suggests that the eclipsing material is extending well beyond the Roche Lobe and that it is probably constantly replenished (see also Bégin 2006). Indeed, under the influence of the MSP intense radiation field, a (otherwise normal) MS star may expand to fill its Roche Lobe (D'antona & Ergma 1993) and even start to lose mass, while the accretion on the pulsar is inhibited by its magnetic pressure (as in the case of MSP-A in NGC 6397; Ferraro et al 2001b; see also Archibald et al. 2009). Moreover Bégin (2006) found a large orbital period derivative for this system, suggesting that the binary is losing material and is spiraling out to longer orbital period.

All these considerations indicate that COM-M28H is a highly-perturbed star which is currently losing mass, and that the system is surrounded by large clouds of gas. Whether or not part of the lost mass was accreted by the NS and served to reaccelerate it in the past (as in the case of J1023+0038; Archibald et al. 2009) cannot be inferred from the available data. We note however that, while from the natural cluster dynamical evolution massive objects are expected to be concentrated close to the centre, M28H is the second most off-centered (after M28F; Bégin et al. 2010) and it is located outside the cluster core. Hence, such an offset position may suggest the following scenario: the NS was recycled by another companion (that eventually became a very low mass, exhausted star, because of the heavy mass transfer); then an exchange interaction occurred in the cluster core between the MSP binary and a MS star, thus causing the ejection of the lightest star and kicking the newly-formed system away from the centre; the new companion started to suffer heavy perturbations (bloating, mass loss, etc.) induced by the MSP and we currently observe it as

[5]Under the assumption of black body radiation (with the luminosity L given by $L \propto R^2 T_{eff}^4$), a $0.2M_\odot$ star heated to the observed temperature ($T_{eff} \sim 6000$ K) and bloated to a radius of $\sim 0.65R_\odot$, has a luminosity which is fully consistent with the observed one. This reinforces the hypothesis that COM-M28H completely filled its Roche Lobe. For sake of comparison, the same object with a radius $R \sim 0.2R_\odot$ (the value expected for a MS $0.2M_\odot$; Marigo et al. 2008), would be a factor of ~ 10 too faint.

COM-M28H; then it eventually will become a helium WD. If the MSP was ejected from the cluster core in an exchange encounter, its current position suggests a relatively recent epoch for the formation of this system, since the expected time for such a heavy system to sink back into the M28 centre should be lower than a few Gyr.

While a spectroscopic follow-up may help to better clarify this scenario, the identification of COM-M28H further increases the number of MSPs with a non-degenerate companion in GCs: 4 out 7 optical counterparts identified so far seem to be MS or sub-giant branch, perturbed stars. This likely indicates that exchange interactions are common events in the dense environments of GC cores and they are quite effective in modifying the "natural" outcomes of the pulsar recycling processes (Freire 2005).

We thank the anonymous referee for the fast and careful reading of the manuscript. This research was supported by Agenzia Spaziale Italiana (under contract ASI-INAF I/009/10/0), by the Istituto Nazionale di Astrofisica (INAF, under contract PRIN-INAF 2008) and by the Ministero dell'Istruzione, dell'Università e della Ricerca. Pulsar research at UBC is supported by an NSERC Discovery Grant and by the CFI.

REFERENCES

Alpar, M. A., Cheng, A. F., Ruderman, M. A., & Shaham, J. 1982, Nature, 300, 728

Archibald, A. M., et al. 2009, Science, 324, 1411

Bailyn, C. D. 1992, ApJ, 392, 519

Bailyn, C. D. 1995, ARA&A, 33, 133

Bégin, S., M.Sc. thesis, Dept. of Physics and Astronomy, University of British Columbia (2006).

Bellini, A., & Bedin, L. R. 2009, PASP, 121, 1419

Bhattacharya, D., & van den Heuvel, E. P. J. 1991, Phys. Rep., 203, 1

Bogdanov, S., Grindlay, J. E., & van den Berg, M. 2005, ApJ, 630, 1029

Bogdanov, S. et al. 2010, ApJsubmitted

Buonanno, R., Buscema, G., Corsi, C. E, Ferraro, I., & Iannicola, G., 1983, A&A, 126, 278

Camilo, F., Lorimer, D. R., Freire, P., Lyne, A. G., & Manchester, R. N. 2000, ApJ, 535, 975

Carretta, E., & Gratton, R. G. 1997, A&AS, 121, 95

Clark, G. W. 1975, ApJ, 199, L143

Cocozza, G., Ferraro, F. R., Possenti, A., Beccari, G., Lanzoni, B., Ransom, S., Rood, R. T., & D'Amico, N. 2008, ApJ, 679, L105

Cudworth, K. M., & Hanson, R. B. 1993, AJ, 105, 168

D'Antona, F., & Ergma, E. 1993, A&A, 269, 219

Davies, M. B., & Hansen, B. M. S. 1998, MNRAS, 301, 15

Edmonds, P. D., Gilliland, R. L., Heinke, C. O., Grindlay, J. E., & Camilo, F. 2001, ApJ, 557, L57

Edmonds, P. D., Gilliland, R. L., Camilo, F., Heinke, C. O., & Grindlay, J. E. 2002, ApJ, 579, 741

Ferraro, F. R., Fusi Pecci, F., & Bellazzini, M. 1995, A&A, 294, 80

Ferraro, F. R., Messineo, M., Fusi Pecci, F., de Palo, M. A., Straniero, O., Chieffi, A., & Limongi, M. 1999, AJ, 118, 1738

Ferraro, F. R., D'Amico, N., Possenti, A., Mignani, R.P., & Paltrinieri, B., 2001a, ApJ, 561, 337

Ferraro, F. R., Possenti, A., D'Amico, N., & Sabbi, E., 2001b, ApJ, 561, L93

Ferraro, F. R., Possenti, A., Sabbi, E., Lagani, P., Rood, R. T., D'Amico, N., & Origlia, L. 2003, ApJ, 595, 179

Ferraro, F. R., Possenti, A., Sabbi, E., & D'Amico, N. 2003, ApJ, 596, L211

Ferraro, F. R., et al. 2009a, Nature, 462, 1028

Ferraro, F. R., et al. 2009b, Nature, 462, 483

Fregeau, J. M. 2008, ApJ, 673, L25

Freire, P. C., Camilo, F., Kramer, M., Lorimer, D. R., Lyne, A. G., Manchester, R. N., & D'Amico, N. 2003, MNRAS, 340, 1359

Freire, P. C. C. 2005, Binary Radio Pulsars, 328, 405

Goodman, J., & Hut, P. 1989, Nature, 339, 40

Harris, W. E. 1996, AJ, 112, 1487

Heggie, D. C. 1975, MNRAS, 173, 729

Hills, J. G., & Day, C. A. 1976, Astrophys. Lett., 17, 87

Holtzman, J. A., Burrows, C. J., Casertano, S., Hester, J. J., Trauger, J. T., Watson, A. M., & Worthey, G. 1995, PASP, 107, 1065

Hut, P., et al. 1992, PASP, 104, 981

Ivanova, N., Heinke, C. O., Rasio, F. A., Belczynski, K., & Fregeau, J. M. 2008, MNRAS, 386, 553

Lanzoni, B., et al. 2007, ApJ, 663, 1040

Lanzoni, B., et al. 2010, ApJ, 717, 653

Lyne, A. G., Brinklow, A., Middleditch, J., Kulkarni, S. R., & Backer, D. C. 1987, Nature, 328, 399

Marigo, P., Girardi, L., Bressan, A., Groenewegen, M. A. T., Silva, L., & Granato, G. L. 2008, A&A, 482, 883

Meylan, G., & Heggie, D. C. 1997, A&A Rev., 8, 1

Paczyński, B. 1971, ARA&A, 9, 183

Phinney, E. S. 1992, Royal Society of London Philosophical Transactions Series A, 341, 39

Pooley, D., et al. 2003, ApJ, 591, L131

Possenti, A., D'Amico, N., Manchester, R. N., Camilo, F., Lyne, A. G., Sarkissian, J., & Corongiu, A. 2003, ApJ, 599, 475

Pryor, C., & Meylan, G. 1993, Structure and Dynamics of Globular Clusters, 50, 357

Ransom, S. M., Hessels, J. W. T., Stairs, I. H., Freire, P. C. C., Camilo, F., Kaspi, V. M., & Kaplan, D. L. 2005, Science, 307, 892

Sigurdsson, S., Richer, H. B., Hansen, B. M., Stairs, I. H., & Thorsett, S. E. 2003, Science, 301, 193

Stairs, I. H., Bégin, S., Ransom, S., Freire, P., Hessels, J., Katz, J., Kaspi, V., & Camilo, F. 2006, Bulletin of the American Astronomical Society, 38, 1118

Stetson, P. B. 1987, PASP, 99, 191

Stetson, P. B. 1994, PASP, 106, 250

Verbunt, F., Bunk, W. H., Ritter, H., & Pfeffermann, E. 1997, A&A, 327, 602

Zinn, R. 1980, ApJS, 42, 19

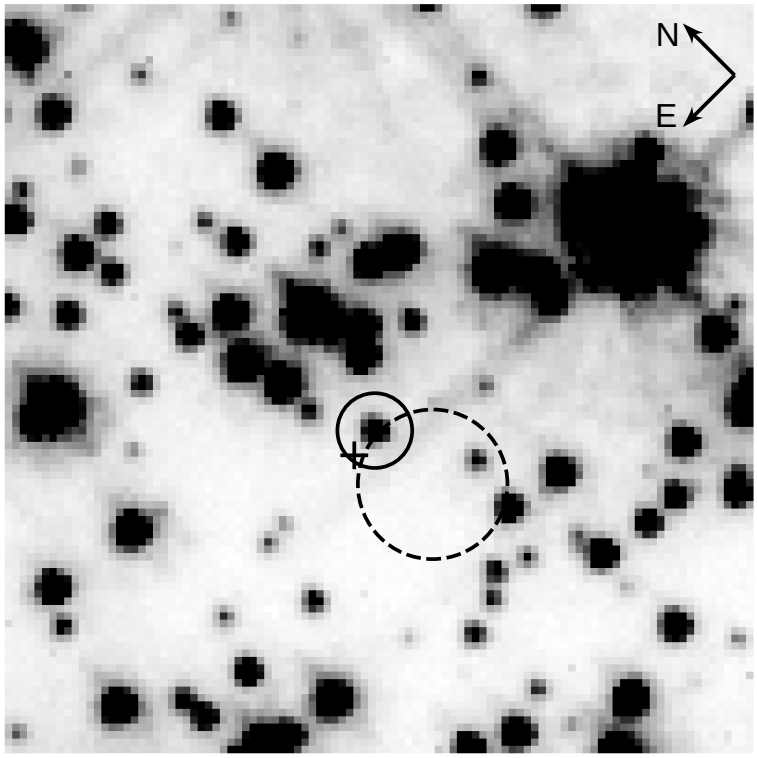

Fig. 1.— U-band, $4'' \times 4''$ WFC3 sub-image of M28 centered on the position of COM-M28H, identified as the companion star to the MSP M28H. The solid circle has a radius of $0.2''$, corresponding to the estimated astrometric accuracy of our analysis. The position of the radio source M28H is marked with the cross. The dashed circle ($0.4''$ radius) marks the position and estimated uncertainty of the X-ray source.

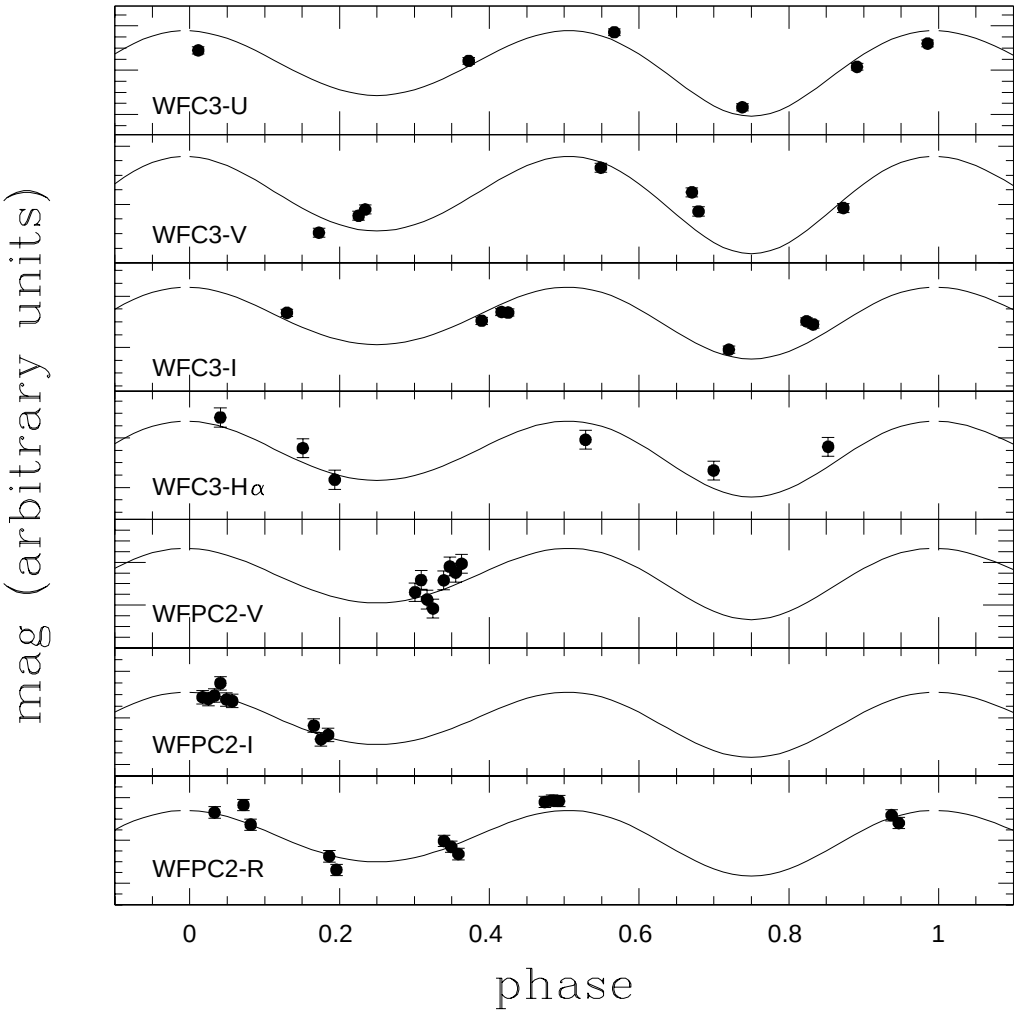

Fig. 2.— The observed light curves in the WFC3 and WFPC2 images. The best fit model is shown as a solid line in each panel.

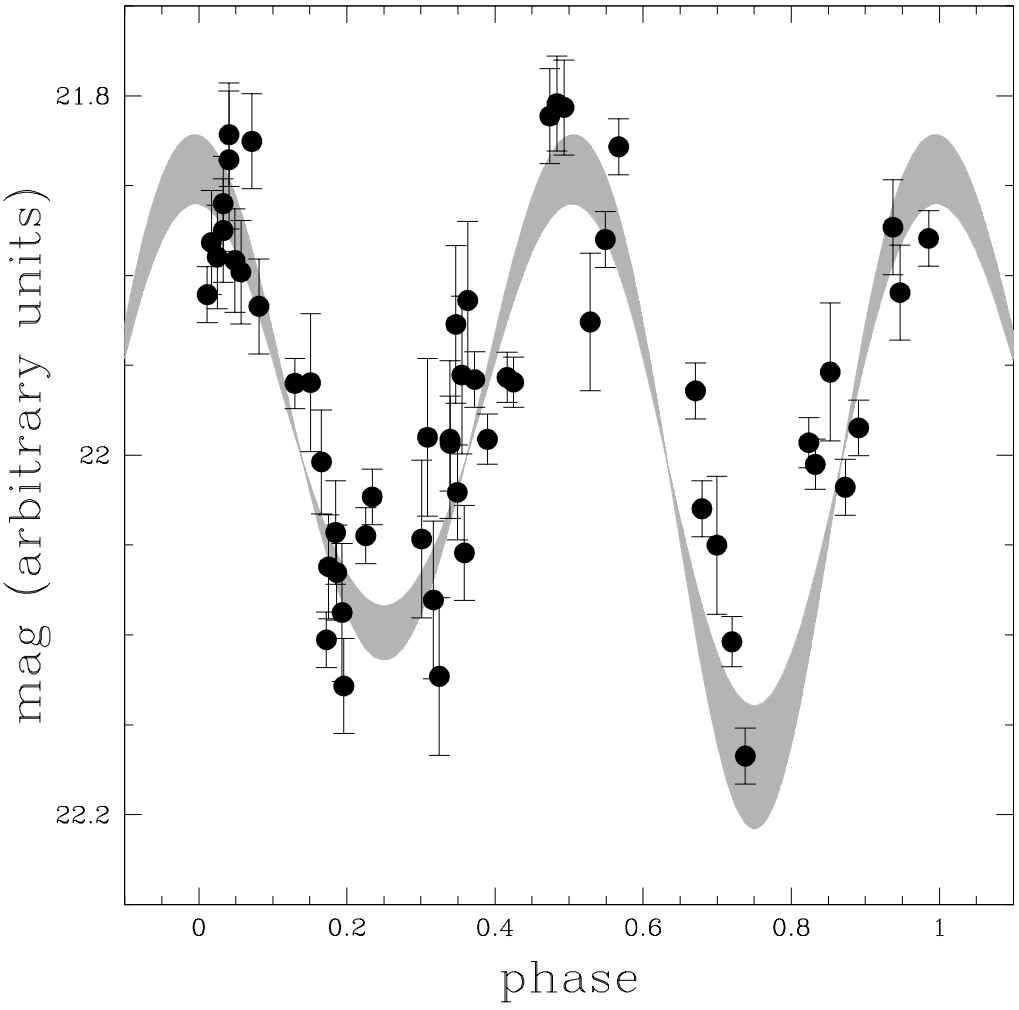

Fig. 3.— The global light curve of COM-M28H, obtained by combining the data points shown in Fig. 2. The grey area represents the region spanned by the best-fit light curves in each photometric band.

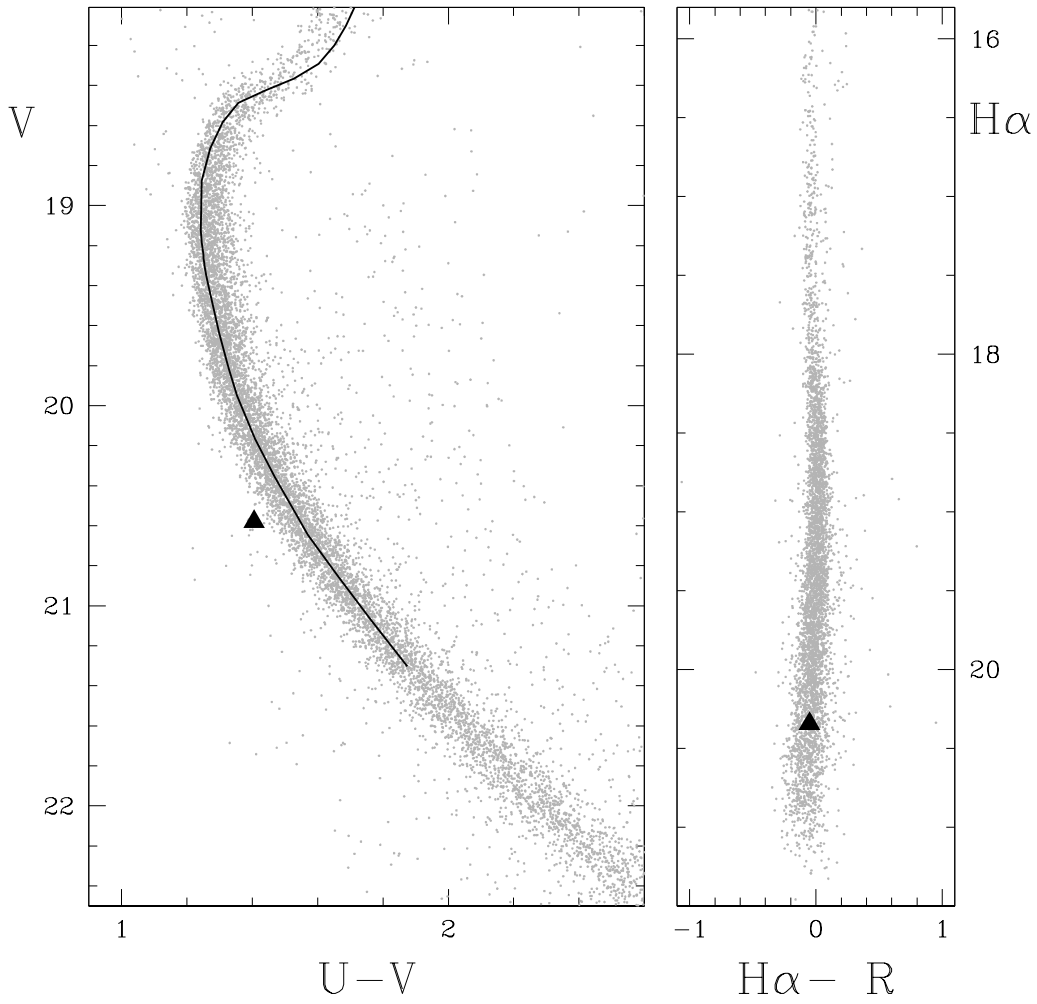

Fig. 4.— CMDs of M28 derived by WFC3 data in a circular region of $\sim 30''$ radius centered on the position of COM-M28H (left panel), and by a combination of WFC3 and WFPC2 data (right panel). The solid triangle marks the position of COM-M28H. The plotted isochrone (from Marigo et al. 2008) has been obtained for $t = 13$ Gyr, [Fe/H]$= -1.27$, $E(B-V) = 0.4$ and (m-M)$_V = 14.97$.

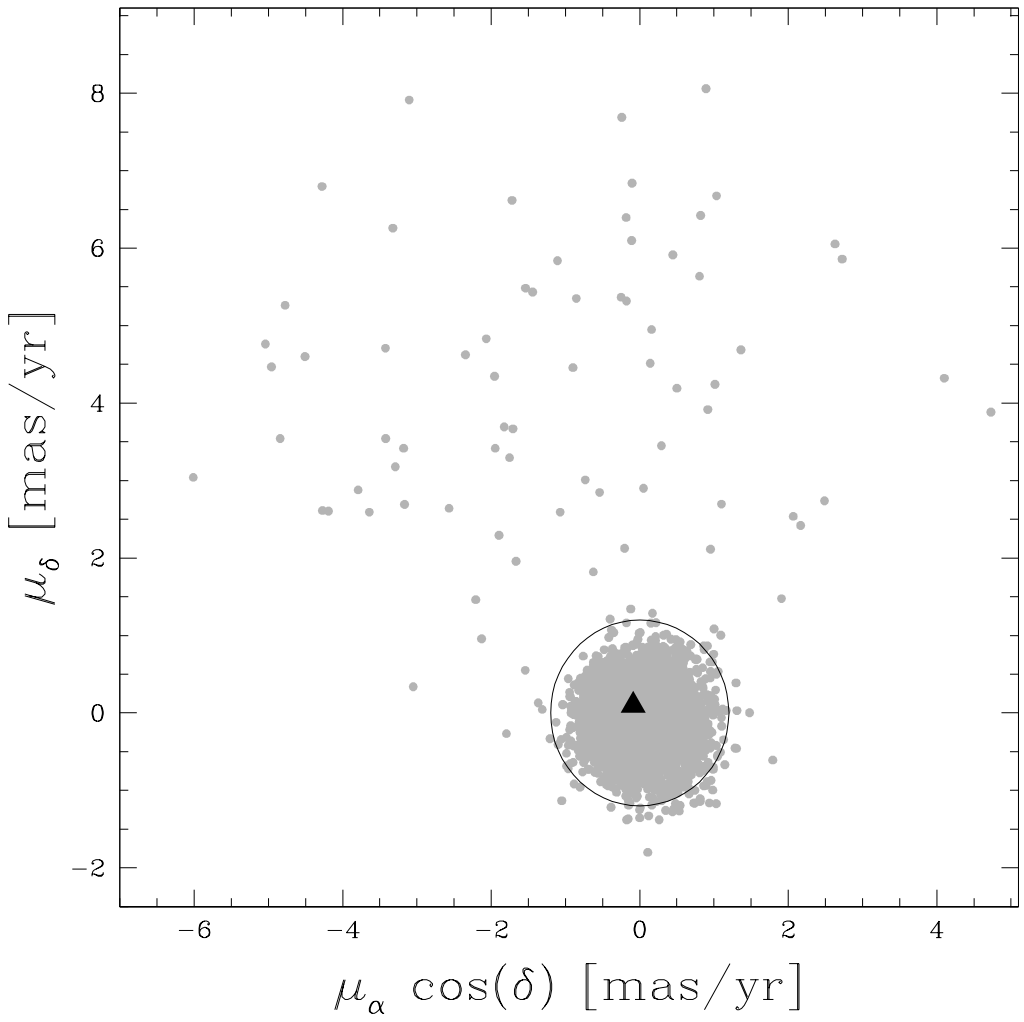

Fig. 5.— Relative proper motion diagram of M28 in equatorial coordinates. The solid triangle represents the position of COM-M28H.